Coordinated Beamforming for Multi-Cell MIMO-NOMA

Wonjae Shin, Mojtaba Vaezi, Byungju Lee, David J. Love, Jungwoo Lee, and H. Vincent Poor

***Abstract*— In this letter, two novel coordinated beamforming techniques are developed to enhance the performance of *non-orthogonal multiple access* combined with multiple-input multiple-output communication in the presence of inter-cell interference. The proposed schemes successfully deal with inter-cell interference, and increase the cell-edge users' throughput, which in turn improves user fairness. In addition, they increase the number of served users, which makes them suitable for 5G networks where massive connectivity and higher spectral efficiency are required. Numerical results confirm the effectiveness of the proposed algorithms.**

***Index Terms*— Non-orthogonal multiple access, inter-cell interference, interference alignment, 5G communications.**

I. Introduction

FUTURE communication networks must support very high throughput, low latency, and massive connectivity. By allowing multiple users to share the same time/frequency, *non-orthogonal* multiple access (NOMA) [1] can address these challenges more efficiently than the conventional *orthogonal* multiple access (OMA) schemes, such as time division multiple access. NOMA exploits the path loss differences amongst the users to separate signals. It increases *spectral efficiency* and *user fairness* by exploiting a capacity-achieving scheme in the downlink. In addition, NOMA supports more connections by letting more than one user simultaneously access the same wireless resources, and reduces latency by allowing grant-free uplink transmission [2].

To achieve high spectral efficiency, NOMA has been combined with multiple-input multiple-output (MIMO) communication [3]–[5] and extended to multi-cell systems [6]. Multi-cell NOMA intensifies inter-cell interference at the boundary of cellular networks, which reduces the quality of service (QoS) for cell-edge users and deteriorates user fairness. To avoid these problems, a coordinated multipoint (CoMP) transmission based scheme is proposed in [7]. CoMP is however demanding in terms of backhaul bandwidth, latency, and computational load due to excessive *data sharing* requirements.

In this letter, we study multi-cell MIMO-NOMA networks in the downlink and propose two *interference alignment* (IA)-based *coordinated beamforming* (CBF) methods in which two base stations (BSs) jointly optimize their beamforming vectors in order to improve the data rates of cell-edge users, without requiring data sharing between cells. Both algorithms use IA-based CBF techniques to cancel inter-cell interference as well as inter-cluster interference, and *successive interference cancellation* (SIC) to cancel intra-cluster interference. These algorithms are termed interfering channel alignment based CBF (ICA-CBF) and IA-based CBF (IA-CBF), respectively. While the former requires full channel state information (CSI) at the BS, the latter only requires the knowledge of cell-edge users' effective serving channel gains at the BS. This can be easily accomplished using single-cell feedback. Thus, IA-CBF imposes much less system overhead compared to ICA-CBF, which requires all users' channel matrices for both serving and interfering links at the BS. We discuss the antenna configurations for which the proposed schemes are feasible.

II. System Model

We consider a two-cell downlink cellular network[1] in which each cell consists of K clusters each consisting of two users: one close to the cell-center and the other close to the cell-edge. Assume each BS and each user has M and N antennas, respectively. In a multi-cell network, cell-edge users experience inter-cell interference whether OMA or NOMA is used. However, this interference situation becomes worse when NOMA is used. This is because in a NOMA-based system, cell-edge users constantly experience interference from the neighboring cell, whereas in the case of OMA interference is limited to certain time slots or frequency bands. A key feature of NOMA is to exploit the difference between users' channel conditions to separate signals in each cluster. Hence, NOMA usually pairs users with good and poor channel conditions in one cluster, by superimposing their signals.

Let $i \in \{\alpha, \beta\}$ and $k \in \mathcal{K} \triangleq \{1, \ldots, K\}$ represent the cell index and the cluster index within each cell, respectively, and $j \in \{1, 2\}$ be the user index in each cluster, where $j = 1$ and $j = 2$, respectively, represent cell-center and cell-edge users. $\mathbf{H}_{j,k}^{[i]}$ and $\mathbf{G}_{j,k}^{[i]}$, respectively, denote the serving and interfering channel matrices of size $N \times M$ for the jth user at the kth cluster of cell i. We assume that all entries of the channel matrices are drawn from a continuous distribution. We also assume that cell-center users do not suffer from inter-cell interference. The received signals at the kth *cell-center*

[1]We consider a two-cell configuration as it is relevant in practice where there is usually one dominant interfering BS. However, the algorithms can be extended to more than two cells.

Manuscript received August 29, 2016; accepted September 23, 2016. Date of publication October 4, 2016; date of current version January 6, 2017. The work of W. Shin and J. Lee was supported in part by the Basic Science Research Program (NRF-2015R1A2A1A15052493) through the National Research Foundation of Korea (NRF) funded by MSIP, the ICT R&D program of MSIP/IITP (IITP-2016-B0717-16-0023), the Bio-Mimetric Robot Research Center funded by DAPA (UD130070ID), INMAC, and BK21-plus. The work of H. V. Poor was supported in part by the U.S. National Science Foundation under Grant EECS-1343210. The associate editor coordinating the review of this letter and approving it for publication was A. Lioumpas. *(Corresponding author: Byungju Lee.)*

W. Shin and J. Lee are with the Department of Electrical and Computer Engineering, Seoul National University, Seoul 08826, South Korea (e-mail: wonjae.shin@snu.ac.kr; junglee@snu.ac.kr).

M. Vaezi and H. V. Poor are with the Department of Electrical Engineering, Princeton University, Princeton, NJ 08544 USA (e-mail: mvaezi@princeton.edu; poor@princeton.edu).

B. Lee and D. J. Love are with the School of Electrical and Computer Engineering, Purdue University, West Lafayette, IN 47907 USA (e-mail: byungjulee@purdue.edu; djlove@purdue.edu).

Digital Object Identifier 10.1109/LCOMM.2016.2615097

and *cell-edge* users of cell i, can be, respectively, expressed as

$$\mathbf{y}_{1,k}^{[i]} = \mathbf{H}_{1,k}^{[i]} \sum_{\ell=1}^{K} \mathbf{x}_{\ell}^{[i]} + \mathbf{z}_{1,k}^{[i]}, \tag{1}$$

$$\mathbf{y}_{2,k}^{[i]} = \mathbf{H}_{2,k}^{[i]} \sum_{\ell=1}^{K} \mathbf{x}_{\ell}^{[i]} + \mathbf{G}_{2,k}^{[i]} \sum_{\ell=1}^{K} \mathbf{x}_{\ell}^{[\bar{i}]} + \mathbf{z}_{2,k}^{[i]}, \tag{2}$$

where $\bar{i} \triangleq \{\alpha, \beta\}\backslash\{i\}$, $\mathbf{x}_k^{[i]}$ is the $M \times 1$ superimposed signal for the kth cluster in BS i and is given by

$$\mathbf{x}_k^{[i]} = \mathbf{v}_k^{[i]} s_k^{[i]} = \mathbf{v}_k^{[i]} \left(\sqrt{\lambda_{1,k}^{[i]}} s_{1,k}^{[i]} + \sqrt{\lambda_{2,k}^{[i]}} s_{2,k}^{[i]} \right), \tag{3}$$

in which $s_{j,k}^{[i]}$ is a data symbol, $\lambda_{j,k}^{[i]}$ is the NOMA power allocation coefficient for the superimposed signal, and $\mathbf{v}_k^{[i]} \in \mathbb{C}^{M\times 1}$ is a *transmit beamformer*. For simplicity of notation, we assume $\lambda_{1,k}^{[i]} + \lambda_{2,k}^{[i]} = 1$ and $\left\|\mathbf{v}_k^{[i]}\right\|_2 = 1$.

III. New CBF Design for Multi-Cell MIMO-NOMA

We propose two novel algorithms to manage the mixture of interference signals for both cell-edge and cell-center users in two-cell MIMO-NOMA networks. In particular, to successfully decode the message of each cell-edge user, we need to cancel inter-cell, inter-cluster, and intra-cluster interference. These are managed by CBF for the first two types of interference, and SIC for the last one. A cell-center user, however, only needs to cancel the latter two types of interference, as it is assumed not to suffer from inter-cell interference.

In both algorithms, the number of transmit antennas at each BS is assumed to be $M = K + 1$. To ensure no inter-cell and inter-cluster interferences, zero-forcing (ZF) transmit beamforming can serve $\left\lfloor \frac{M+1}{3} \right\rfloor$ clusters which is much less than K clusters [5]. To overcome this problem, interference alignment is applied in the following subsections so that the number of served clusters in each cell remains close to M even in the presence of inter-cell interference, similar to that in single-cell NOMA [5]. To make the exposition concrete, we focus on beamforming design in cell α.[2]

A. Algorithm I: ICA-CBF NOMA

Consider the case in which $M = K + 1$ and $N = K$, and assume that full CSI is available at each BS.[3] A receive beamformer can be constructed to align the *effective interfering channels* for a given cell within a one-dimensional space. That is, through the interfering channel alignment, each BS can regard K distinct interfering channels as a single one-dimensional channel, which allows more clusters in each cell for a certain number of transmit antennas. We can find such *receive beamformers* $\mathbf{w}_{2,1}^{[\alpha]}, \ldots, \mathbf{w}_{2,K}^{[\alpha]} \in \mathbb{C}^{N\times 1}$ and aligned interfering channel $\boldsymbol{\tau}^{[\alpha]} \in \mathbb{C}^{M\times 1}$ by solving the following matrix equation:

$$\begin{bmatrix} -\mathbf{I}_M & \mathbf{G}_{2,1}^{[\alpha]\dagger} & \mathbf{0} & \cdots & \mathbf{0} \\ -\mathbf{I}_M & \mathbf{0} & \mathbf{G}_{2,2}^{[\alpha]\dagger} & \cdots & \mathbf{0} \\ \vdots & \vdots & \ddots & \ddots & \vdots \\ -\mathbf{I}_M & \mathbf{0} & \cdots & \mathbf{0} & \mathbf{G}_{2,K}^{[\alpha]\dagger} \end{bmatrix} \begin{bmatrix} \boldsymbol{\tau}^{[\alpha]} \\ \mathbf{w}_{2,1}^{[\alpha]} \\ \mathbf{w}_{2,2}^{[\alpha]} \\ \vdots \\ \mathbf{w}_{2,K}^{[\alpha]} \end{bmatrix} = \mathbf{0}, \tag{4}$$

[2]By symmetry, it is straightforward to extend the result of cell α to cell β.

[3]The algorithm is feasible for any $M \geq K + 1$ and $N \geq K$, though.

where $(\mathbf{A})^{\dagger}$ denotes the complex conjugate and transpose of $\mathbf{A}$. Since the size of the unified matrix in the left-hand side of (4) is $KM \times (M + KN)$ and all elements of $\mathbf{G}_{2,k}^{[\alpha]}$ come from a continuous random distribution, it follows that the unified matrix has a full-rank of $KM{=}K(K+1)$ almost surely. Thus, it is possible to find $\mathbf{w}_{2,1}^{[\alpha]}, \ldots, \mathbf{w}_{2,K}^{[\alpha]}$ and $\boldsymbol{\tau}^{[\alpha]}$ in the null space of the unified matrix almost surely.

Subsequently, the *transmit beamformers* $\mathbf{v}_k^{[\alpha]}$ at BS α can be designed to ensure zero inter-cell and inter-cluster interference at the cell-edge users as

$$\mathbf{v}_k^{[\alpha]} \perp \begin{bmatrix} \boldsymbol{\tau}^{[\beta]\dagger} \\ \bar{\mathbf{H}}_{2,k}^{[\alpha]} \end{bmatrix}^{\dagger}, \tag{5}$$

where $\bar{\mathbf{H}}_{2,k}^{[\alpha]}$ is a $(K-1)\times(K+1)$ matrix obtained by removing the kth row of $\mathbf{H}_2^{[\alpha]} = \left[\mathbf{H}_{2,1}^{[\alpha]\dagger}\mathbf{w}_{2,1}^{[\alpha]} \cdots \mathbf{H}_{2,K}^{[\alpha]\dagger}\mathbf{w}_{2,K}^{[\alpha]}\right]^{\dagger}$ and $\mathbf{a} \perp \mathbf{A}$ denotes that $\mathbf{a}$ is orthogonal to the subspace spanned by the columns of $\mathbf{A}$. Recall from (4) that the receive beamformer $\mathbf{w}_{2,k}^{[\alpha]}$ is designed independently of the channel matrix $\mathbf{H}_{2,k}^{[\alpha]}$. Also, the elements of the effective channel vectors $\mathbf{H}_{2,k}^{[\alpha]\dagger}\mathbf{w}_{2,k}^{[\alpha]}$ and $\mathbf{H}_{2,\bar{k}}^{[\alpha]\dagger}\mathbf{w}_{2,\bar{k}}^{[\alpha]}$ for $\bar{k} \in \mathcal{K}\backslash\{k\}$ are statistically independent random variables. Moreover, the aligned interfering channel $\boldsymbol{\tau}^{[\beta]}$ is a function of $\mathbf{G}_{2,k}^{[\beta]}$ only, but not $\mathbf{H}_{2,k}^{[\alpha]}$ or $\mathbf{G}_{2,k}^{[\alpha]}$. This implies that all the column vectors of $\left[\boldsymbol{\tau}^{[\beta]} \;\; \bar{\mathbf{H}}_2^{[\alpha]\dagger}\right]$ are linearly independent almost surely, and it is possible to find the precoding vector $\mathbf{v}_k^{[\alpha]}$ in the null space of the matrix, for any $k \in \mathcal{K}$.

Recall that the cell-center users are assumed not to suffer from interference caused by the neighboring cells. With this assumption, the cell-center users only need to remove the inter-cluster interference caused by the other $K-1$ clusters within that cell. This can be accomplished by a ZF decoder with K receive antennas, i.e.,

$$\mathbf{w}_{1,k}^{[\alpha]} \perp \mathbf{H}_{1,k}^{[\alpha]} \left[\mathbf{v}_1^{[\alpha]} \; \ldots \; \mathbf{v}_{k-1}^{[\alpha]} \; \mathbf{v}_{k+1}^{[\alpha]} \; \ldots \; \mathbf{v}_K^{[\alpha]}\right]. \tag{6}$$

Thus, with the help of ICA-CBF we can equivalently decompose the two-cell MIMO-NOMA channels into $2K$ pairs of single-antenna NOMA channels. In particular, the received signals at a cell-center user ($j = 1$) and cell-edge user ($j = 2$) of the kth cluster in cell α are given by

$$\mathbf{w}_{j,k}^{[\alpha]\dagger}\mathbf{y}_{j,k}^{[\alpha]} = \tilde{h}_{j,k}^{[\alpha]} \left(\sqrt{\lambda_{1,k}^{[\alpha]}} s_{1,k}^{[\alpha]} + \sqrt{\lambda_{2,k}^{[\alpha]}} s_{2,k}^{[\alpha]} \right) + \tilde{z}_{j,k}^{[\alpha]}, \tag{7}$$

where $\tilde{h}_{j,k}^{[\alpha]} = \mathbf{w}_{j,k}^{[\alpha]\dagger}\mathbf{H}_{j,k}^{[\alpha]}\mathbf{v}_k^{[\alpha]}$ and $\tilde{z}_{j,k}^{[\alpha]} = \mathbf{w}_{j,k}^{[\alpha]\dagger}\mathbf{z}_{j,k}^{[\alpha]}$ are, respectively, the effective serving channel coefficient and effective noise term after applying transmit/receive beamforming. Therefore, for a cell-center user, intra-cluster interference can be decoded and cancelled using SIC so that the desired message is decoded free of interference. The cell-edge users, however, decode their messages by treating the intra-cluster interference as noise [1].

B. Algorithm II: IA-CBF NOMA

Now, consider a more realistic scenario with $M = N = K + 1$ where CSI is available only for the serving channels of each BS via single-cell feedback. To reduce the overhead of channel estimation and uplink feedback, we can apply *cascaded transmit beamforming* [8] in two-cell MIMO-NOMA,

in which the inner precoder is predetermined with no prior information and the outer precoder is implemented using the effective serving channel vectors. Specifically, the transmit beamformers can be designed as

$$\mathbf{v}_k^{[i]} = \mathbf{P}^{[i]}\mathbf{f}_k^{[i]}, \quad \forall i, k, \tag{8}$$

where $\mathbf{P}^{[i]} \in \mathbb{C}^{M\times K}$ indicates the inner precoder for cell i,[4] and $\mathbf{f}_k^{[i]} \in \mathbb{C}^{K\times 1}$ denotes the outer precoder for the users in the kth cluster of cell i.

Notice that $\mathbf{G}_{2,k}^{[\alpha]}\mathbf{P}^{[\beta]}\mathbf{f}_\ell^{[\beta]} \in \text{span}\big(\mathbf{G}_{2,k}^{[\alpha]}\mathbf{P}^{[\beta]}\big)$, $\forall k, \ell \in \mathcal{K}$, regardless of the value of $\mathbf{f}_\ell^{[\beta]}$; thereby, $\text{span}\big(\mathbf{G}_{2,k}^{[\alpha]}\mathbf{P}^{[\beta]}\big)$ can be termed the *aligned interference subspace* at the cell-edge user of the kth cluster in cell α. Each cell-edge user in cell α can estimate the K-dimensional aligned interference subspace, guaranteeing a one-dimensional space free of interference for its corresponding cluster's signal. Thus, the receive beamformers for the cell-edge user can be designed as

$$\mathbf{w}_{2,k}^{[\alpha]} \perp \mathbf{G}_{2,k}^{[\alpha]}\mathbf{P}^{[\beta]}, \quad \forall k, \tag{9}$$

which guarantees that

$$\mathbf{w}_{2,k}^{[\alpha]^\dagger}\mathbf{G}_{2,k}^{[\alpha]}\mathbf{v}_k^{[\beta]} = \underbrace{\mathbf{w}_{2,k}^{[\alpha]^\dagger}\mathbf{G}_{2,k}^{[\alpha]}\mathbf{P}^{[\beta]}}_{=\mathbf{0}}\mathbf{f}_k^{[\beta]} = 0. \tag{10}$$

To cancel all the inter-cluster interference for all K cell-edge users in cell α, it suffices for $\mathbf{f}_k^{[\alpha]}$ to satisfy

$$\mathbf{w}_{2,k}^{[\alpha]^\dagger}\mathbf{H}_{2,\bar{k}}^{[\alpha]}\mathbf{P}^{[\alpha]}\mathbf{f}_{\bar{k}}^{[\alpha]} = 0, \quad \forall \bar{k} \in \mathcal{K}\backslash\{k\} \tag{11}$$

or equivalently

$$\mathbf{f}_k^{[\alpha]} \perp \mathbf{P}^{[\alpha]^\dagger}\bar{\mathbf{H}}_{2,k}^{[\alpha]}. \tag{12}$$

Note that no information about the interfering channels is required to determine the precoder $\mathbf{v}_k^{[\alpha]} = \mathbf{P}^{[\alpha]^\dagger}\mathbf{f}_k^{[\alpha]}$ for the cell-edge users since BS α does not need to acquire any $\mathbf{G}_{j,k}^{[i]}$ in order to construct $\mathbf{f}_k^{[\alpha]}$ for a given $\mathbf{P}^{[i]}$, as seen in (11).

For cell-center users, a similar approach to receive beamforming for a single-cell MIMO-NOMA [4] is applied so that the receive beamforming vector can be represented as a product of two matrices, i.e.,

$$\mathbf{w}_{1,k}^{[\alpha]} = \mathbf{Q}_{1,k}^{[\alpha]}\mathbf{c}_k^{[\alpha]}, \tag{13}$$

where $\mathbf{Q}_{1,k}^{[\alpha]} \in \mathbb{C}^{M\times 2}$ is a matrix consisting of those *left singular vectors* of $\mathbf{H}_{1,k}^{[\alpha]}\mathbf{P}^{[\alpha]}\big[\mathbf{f}_1^{[\alpha]}\cdots\mathbf{f}_{k-1}^{[\alpha]}\,\mathbf{f}_{k+1}^{[\alpha]}\cdots\mathbf{f}_K^{[\alpha]}\big] \in \mathbb{C}^{M\times(M-2)}$ which correspond to its zero singular values. Then, the constraint

$$\mathbf{w}_{1,k}^{[\alpha]^\dagger}\mathbf{H}_{1,k}^{[\alpha]}\mathbf{v}_{\bar{k}}^{[\alpha]} = \mathbf{c}_k^{[\alpha]^\dagger}\underbrace{\mathbf{Q}_{1,k}^{[\alpha]^\dagger}\mathbf{H}_{1,k}^{[\alpha]}\mathbf{P}^{[\alpha]}\mathbf{f}_{\bar{k}}^{[\alpha]}}_{=\mathbf{0}} = 0, \quad \forall \bar{k} \in \mathcal{K}\backslash\{k\},$$

should be satisfied. Further, to maximize the serving channel gain while guaranteeing no inter-cluster interference, maximal ratio combining can be applied to $\mathbf{c}_k^{[\alpha]}$ as in [4], to get

$$\mathbf{c}_k^{[\alpha]} = \mathbf{Q}_{1,k}^{[\alpha]^\dagger}\mathbf{H}_{1,k}^{[\alpha]}\mathbf{v}_k^{[\alpha]} \big/ \big\|\mathbf{Q}_{1,k}^{[\alpha]^\dagger}\mathbf{H}_{1,k}^{[\alpha]}\mathbf{v}_k^{[\alpha]}\big\|_2. \tag{14}$$

[4]The inner precoders can be the same across cells, i.e., $\mathbf{P}^{[\alpha]} = \mathbf{P}^{[\beta]}$ whose elements are independent of channel gains.

TABLE I

COMPARISON BETWEEN THE PROPOSED NOMA ALGORITHMS AND EXISTING NOMA AND OMA SCHEMES

Algorithm	# of Tx antennas	# of Rx antennas	# of served users	CSI at BS
OMA [4]	K	K	K	No
NOMA [4]	K	K	$2K$	No
SA-NOMA [5]	K	$\lceil\frac{K}{2}+1\rceil$	$2K$	Full
IA-CBF NOMA	K+1	K+1	$4K$	Partial
ICA-CBF NOMA	K+1	K	$4K$	Full

When the BS and its corresponding users apply the transmit and receive beamformers based on IA-CBF, $\mathbf{v}_k^{[i]}$ and $\mathbf{w}_{j,k}^{[i]}$, respectively, the two-cell MIMO-NOMA channel can be decomposed into $2K$ pairs of single-antenna NOMA channels with no inter-cell or inter-cluster interference. As the last step, the SIC strategy can be applied to decode the users' messages similar to ICA-CBF case. As a final note, it is emphasized that the algorithm is valid for any $M, N \geq K+1$.

C. Discussion

In this subsection, we briefly discuss the key distinctions of the proposed CBF-based NOMA schemes from the existing NOMA and OMA schemes. Recall that there are $2K$ users in each cell. Thus, OMA needs two time slots so that K users are simultaneously served in each time slot [4]. On the other hand, NOMA-based schemes can simultaneously support $2K$ users by transmitting superimposed messages [4]. When the full CSI is available at the BS, a signal alignment (SA) technique can be exploited to effectively manage intra-cell interference [5]; thereby the required number of receive antennas can be further reduced by SA-NOMA, especially when $K \geq 4$. As mentioned above, the proposed CBF algorithms can effectively mitigate the intra-cell and inter-cell interference with a slightly higher number of antennas, resulting in simultaneous support of $4K$ users over the same wireless resources. Notice that ICA-CBF NOMA achieves the same number of served users as that of IA-CBF NOMA although it operates with a smaller number of receive antennas. Table I summarizes the required numbers of transmit/receive antennas to support a certain number of users in each scheme.

Remark 1 (Support of Massive Connectivity): When K is large, the number of extra antennas required for the proposed CBF-based NOMA becomes negligible. That is, without significantly many additional antenna elements, the number of served users for the proposed algorithms has increased by factors of four and two compared to OMA and NOMA, respectively. Therefore, the proposed algorithms can support connectivity for a very large number of devices using only a limited amount of wireless resources (i.e., low-cost and low-energy).

IV. NUMERICAL RESULTS

In this section, we compare the performance of the proposed algorithms with existing NOMA and OMA schemes. We deploy a two-cell network in which K clusters are served in each cell. Each cluster consists of two users having very different channel conditions. We assume that the cell-center users are deployed within the area of a disc with radius r_A. The cell-edge users are deployed within the ring-shaped area

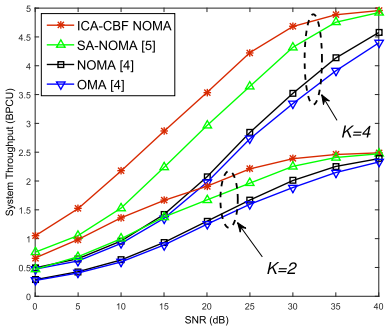

Fig. 1. The performance of ICA-CBF NOMA with different numbers of clusters K for $M = K + 1$, $N = K$, $r_A = 2$m, $r_B = 8$m, $r_C = 10$m.

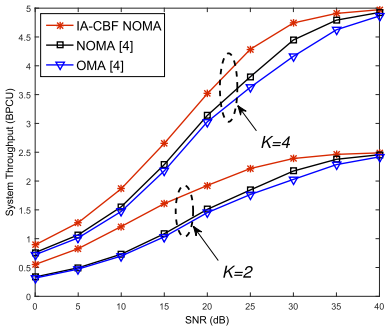

Fig. 2. The performance of IA-CBF NOMA with different numbers of clusters K for $M = N = K + 1$, $r_A = 2$m, $r_B = 8$m, $r_C = 10$m.

between a circle with radius r_B and a circle with radius r_C (assuming $r_C > r_B \gg r_A$ [9]). Then, the two users (one from the disk and the other from the ring) are randomly paired to form a cluster.[5] Based on this model, we further assume that the cell-center users do not suffer from inter-cell interference due to the fact that they are far away from the neighboring BS. The path loss exponent is set to 3. As a performance metric, we measure the (per-cell) system throughput [5], [9], which is

$$R = \sum_{k=1}^{K} \Big[R_{1,k} \left(1 - P_{1,k}\right) + R_{2,k} \left(1 - P_{2,k}\right) \Big], \qquad (15)$$

where $R_{1,k}$ and $R_{2,k}$ are the target data rates for the cell-center and cell-edge users in the kth cluster, and $P_{1,k}$ and $P_{2,k}$ are their corresponding outage probabilities, respectively. It can be noted that the metric corresponds to delay-sensitive throughput which measures the rate of successful data transmission. We set the target data rates for the cell-center user and cell-edge user at $R_{1,k} = 1$ bit per channel use (BPCU) and $R_{2,k} = 0.25$ BPCU, for $\forall k \in \mathcal{K}$, respectively.

We plot the system throughput versus signal-to-noise (SNR) with different numbers of clusters in Figs. 1 and 2. In general, one can observe that the system throughput of all the schemes approaches $\sum_{k=1}^{K} \left(R_{1,k} + R_{2,k}\right)$ as the SNR increases. This is because the system throughput is determined only by the targeted data rate in the high SNR regime. We divide our simulation environments into two scenarios according to the availability of the full CSI at the BS. In Fig. 1, we assume that the proposed ICA-CBF NOMA has full CSI (i.e., the $(K+1)\times(K+1)$ channel matrix of all the cell-edge and cell-center users) of the serving as well as interfering cell. We also compare the performance of ICA-CBF NOMA with that of NOMA with full CSI (i.e., SA-NOMA). In our simulations, we use the cognitive radio (CR) inspired power allocation for ICA-CBF NOMA and SA-NOMA with the help of full CSI at the BS [4] It is worth mentioning that the BS can allocate a minimal transmission power in order to meet the cell-edge user's QoS requirement, and then allocate the remaining power to the cell-center user. This CR inspired power allocation can utilize the transmission power more efficiently compared to fixed power allocation, resulting in an increased system throughput. It is observed that the system throughput gains at 20 dB of ICA-CBF NOMA over SA-NOMA and NOMA are 14% and 47% for $K = 2$ and 19% and 71% for $K = 4$. As can be seen from Fig. 1, when the number of clusters K increases, the use of the degrees of freedom at the BS becomes effective and thus the system throughput of ICA-CBF NOMA improves drastically.

In order to show the effectiveness of the proposed algorithm in a realistic scenario, in Fig. 2, we assume that the proposed IA-CBF NOMA has access to only reduced-dimension CSI (i.e., $K \times 1$ effective serving channel vectors of the cell-edge users) of the serving cell while the existing NOMA and OMA schemes have no CSI at the BS. Since it is not possible to measure the QoS requirement with limited CSI at the BS, we use the fixed power allocation of $\lambda_{1,k}^{[i]} = \frac{1}{4}$ and $\lambda_{2,k}^{[i]} = \frac{3}{4}$, for $\forall k \in \mathcal{K}$. It can be observed from this figure that IA-CBF NOMA achieves the best system throughput since it has the lowest outage probability compared with the NOMA and OMA schemes at a certain SNR. Note that IA-CBF NOMA avoids making all the users feed back their CSI to the BS at the cost of only a slight increase in the number of receive antennas.

[5]The use of more sophisticated user-pairing can further improve the system performance [10], [11].

REFERENCES

[1] Y. Saito, Y. Kishiyama, A. Benjebbour, T. Nakamura, A. Li, and K. Higuchi, "Non-orthogonal multiple access (NOMA) for cellular future radio access," in *Proc. IEEE 77th VTC Spring*, Jun. 2013, pp. 1–5.

[2] L. Dai, B. Wang, Y. Yuan, S. Han, C.-L. I, and Z. Wang, "Non-orthogonal multiple access for 5G: Solutions, challenges, opportunities, and future research trends," *IEEE Commun. Mag.*, vol. 53, no. 9, pp. 74–81, Sep. 2015.

[3] Q. Sun, S. Han, C.-L. I, and Z. Pan, "On the ergodic capacity of MIMO NOMA systems," *IEEE Wireless Commun. Lett.*, vol. 4, no. 4, pp. 405–408, Aug. 2015.

[4] Z. Ding, F. Adachi, and H. V. Poor, "The application of MIMO to non-orthogonal multiple access," *IEEE Trans. Wireless Commun.*, vol. 15, no. 1, pp. 537–552, Jan. 2016.

[5] Z. Ding, R. Schober, and H. V. Poor, "A general MIMO framework for NOMA downlink and uplink transmission based on signal alignment," *IEEE Trans. Wireless Commun.*, vol. 15, no. 6, pp. 4438–4454, Jun. 2016.

[6] S. Han, C.-L. I, Z. Xu, and Q. Sun, "Energy efficiency and spectrum efficiency co-design: From NOMA to network NOMA," *MMTC E-Letter*, vol. 9, no. 5, pp. 21–24, Sep. 2014.

[7] J. Choi, "Non-orthogonal multiple access in downlink coordinated two-point systems," *IEEE Commun. Lett.*, vol. 18, no. 2, pp. 313–316, Feb. 2014.

[8] C. Suh, M. Ho, and D. N. C. Tse, "Downlink interference alignment," *IEEE Trans. Commun.*, vol. 59, no. 9, pp. 2616–2626, Sep. 2011.

[9] Y. Liu, Z. Ding, M. Elkashlan, and H. V. Poor, "Cooperative non-orthogonal multiple access with simultaneous wireless information and power transfer," *IEEE J. Sel. Areas Commun.*, vol. 34, no. 4, pp. 938–953, Apr. 2016.

[10] Z. Ding, P. Fan, and H. V. Poor, "Impact of user pairing on 5G non-orthogonal multiple access downlink transmissions," *IEEE Trans. Veh. Technol.*, vol. 65, no. 8, pp. 1462–1465, Aug. 2016.

[11] Y. Liu, M. Elkashlan, Z. Ding, and G. K. Karagiannidis, "Fairness of user clustering in MIMO non-orthogonal multiple access systems," *IEEE Commun. Lett.*, vol. 20, no. 7, pp. 1465–1468, Jul. 2016.